

# Nonselective Currents and Channels in Plasma Membranes of Protoplasts from Coats of Developing Seeds of Bean<sup>1</sup>

Wen-Hao Zhang<sup>2\*</sup>, Martha Skerrett, N. Alan Walker, John W. Patrick, and Stephen D. Tyerman<sup>2</sup>

School of Biological Sciences, The Flinders University of South Australia, G.P.O. Box 2100, Adelaide, South Australia 5001, Australia (W.-H.Z., M.S., S.D.T.); Biophysics Department, School of Physics, The University of New South Wales, Kensington, New South Wales 2052, Australia (N.A.W.); and School of Biological and Chemical Sciences, The University of Newcastle, Newcastle, New South Wales 2308, Australia (W.-H.Z., J.W.P.)

In developing bean (*Phaseolus vulgaris*) seeds, phloem-imported nutrients move in the symplast from sieve elements to the ground parenchyma cells where they are transported across the plasma membrane into the seed apoplast. To study the mechanisms underlying this transport, channel currents in ground parenchyma protoplasts were characterized using patch clamp. A fast-activating outward current was found in all protoplasts, whereas a slowly activating outward current was observed in approximately 25% of protoplasts. The two currents had low selectivity for univalent cations, but the slow current was more selective for K<sup>+</sup> over Cl<sup>-</sup> ( $P_K:P_{Cl} = 3.6\text{--}4.2$ ) than the fast current ( $P_K:P_{Cl} = 1.8\text{--}2.5$ ) and also displayed Ca<sup>2+</sup> selectivity. The slow current was blocked by Ba<sup>2+</sup>, whereas both currents were blocked by Gd<sup>3+</sup> and La<sup>3+</sup>. Efflux of K<sup>+</sup> from seed coat halves was inhibited 25% by Gd<sup>3+</sup> and La<sup>3+</sup> but was stimulated by Ba<sup>2+</sup> and Cs<sup>+</sup>, suggesting that only the fast current may be a component in the pathway for K<sup>+</sup> release. An "instantaneous" inward current observed in all protoplasts exhibited similar pharmacology and permeability for univalent cations to the fast outward current. In outside-out patches, two classes of depolarization-activated cation-selective channels were observed: one slowly activating of low conductance (determined from nonstationary noise to be 2.4 pS) and another with conductances 10-fold higher. Both channels occurred at high density. The higher conductance channel in 10 mM KCl had  $P_K:P_{Cl} = 2.8$ . Such nonselective channels in the seed coat ground parenchyma cell could function to allow some of the efflux of phloem-imported univalent ions into the seed apoplast.

In developing seeds of grain legumes, there is no symplastic continuity between the maternal seed coat and the enclosed embryo (Patrick and Offler, 1995). Thus, all nutrients accumulated by the embryo must cross two plasma membranes: the first between the seed coat symplast and the seed apoplast and the second between the apoplast and the cotyledon symplast (Patrick and Offler, 1995). As a consequence, nutrient transport across membranes is an important process in the transfer of nutrients to embryos. In bean (*Phaseolus vulgaris*), phloem-imported nutrients move through the seed coat symplast from the sieve elements to specialized ground parenchyma cells through whose plasma membranes they are transported to the seed apoplast (Offler and Patrick, 1984; Wang et al., 1995). Suc, K<sup>+</sup>, Cl<sup>-</sup>, and amino nitrogen are the principal nutrients transported by this route (Patrick, 1984; Walker et al., 1995). Suc efflux is char-

acterized by both passive and energy-coupled components, the latter mediated by proton-Suc antiport (Walker et al., 1995, 2000). Passive transport through channels is expected to mediate the efflux of ions from the seed coat symplast to the seed apoplast (Walker et al., 1995; Zhang et al., 1997).

The plasma membranes of plant cells are dominated by two classes of voltage-dependent K<sup>+</sup> channels: slowly activating outward and inward rectifying channels (Maathuis et al., 1997). These K<sup>+</sup> channels are sensitive to tetraethylammonium (TEA<sup>+</sup>), Ba<sup>2+</sup>, and Cs<sup>+</sup>, and are involved in a number of important physiological processes (Maathuis et al., 1997). In addition to these slowly activating and time-dependent K<sup>+</sup> currents, an "instantaneously activating" current has been observed in various types of plant cells. These include maize (*Zea mays*) root cortical and stele cells (Roberts and Tester, 1995, 1997), wheat (*Triticum aestivum*) root cortical cells (Tyerman et al., 1997; Buschmann et al., 2000), and rye (*Secale cereale*) root epidermal cells (White and Lemtiri-Chlieh, 1995). The "instantaneous" current is often weakly rectified and behaves nonselectively for the transport of univalent cations including K<sup>+</sup>, NH<sub>4</sub><sup>+</sup>, Na<sup>+</sup>, and Cs<sup>+</sup> (White and Lemtiri-Chlieh, 1995; Roberts and Tester, 1997; Tyerman et al., 1997;

<sup>1</sup> This work was supported by the Australian Research Council.

<sup>2</sup> Present address: Horticulture, Viticulture, and Oenology, Adelaide University, PMB#1 Glen Osmond, South Australia 5064, Australia.

\* Corresponding author; e-mail wen-hao.zhang@adelaide.edu.au; fax 61-8-83037116.

Article, publication date, and citation information can be found at [www.plantphysiol.org/cgi/doi/10.1104/pp.010566](http://www.plantphysiol.org/cgi/doi/10.1104/pp.010566).

Buschmann et al., 2000). This nonselective cation channel is insensitive to plant  $K^+$  channel blockers,  $TEA^+$ , and  $Cs^+$ , but is inhibited by divalent cations (White and Lemtiri-Chlieh, 1995; Roberts and Tester, 1997; Tyerman et al., 1997). Similar pharmacological characteristics are exhibited in an artificial bilayer by nonselective cation channels from plasma membrane extracted from wheat roots (Davenport and Tester, 2000).

Univalent cation and anion efflux from plant cells could occur through ion channels that are poorly selective between ions of the same charge, or even poorly selective between cations and anions (Wegner and De Boer, 1997). To investigate these issues, we applied the patch clamp technique to protoplasts derived from ground parenchyma cells from the seed coat of developing bean seeds. We anticipated that cation channels would be present that open at depolarized membrane potentials to allow efflux. Because the selectivity for imported nutrients to the seed would most likely occur during phloem loading, we also expected that their selectivity might be low. We have characterized two types of outwardly directed current that exhibit low selectivity between univalent cations, and also between  $K^+$  and  $Cl^-$ . These features of the outward currents would enable the ground parenchyma cells to rapidly release phloem-imported nutrient ions to the seed apoplast.

## RESULTS

### Identification of Protoplasts

Anatomical and physiological studies show that efflux of solutes from coats to the seed apoplast of developing bean seeds occurs from their ground parenchyma cells (Offler and Patrick, 1984; Wang et al., 1995). The impermeant sulfhydryl fluorochrome bromobimane binds selectively to ground parenchyma cells of bean seed coats (Wang et al., 1995). This finding was used to identify their protoplasts. Ground parenchyma cells were tagged in situ with bromobimane and then protoplasts were prepared. Those protoplasts that were labeled with bromobimane (Fig. 1B) exhibited a number of distinctive characteristics including a granulated cytoplasm, relatively large nucleus, off-center vacuole, and lack of chloroplasts (Fig. 1A). These characteristics were subsequently used to select protoplasts for patch clamping in the absence of bromobimane.

### Whole-Cell Outward Current

Membrane depolarization evoked two types of outward current with distinct activation kinetics. A fast-activating outward current was observed in all patched protoplasts ( $n = 202$ ; Fig. 2A), whereas in 25% of protoplasts a slowly activating outward current appeared (Fig. 2B). The fast and slow currents were observed in both low and high  $Cl^-$  pipette

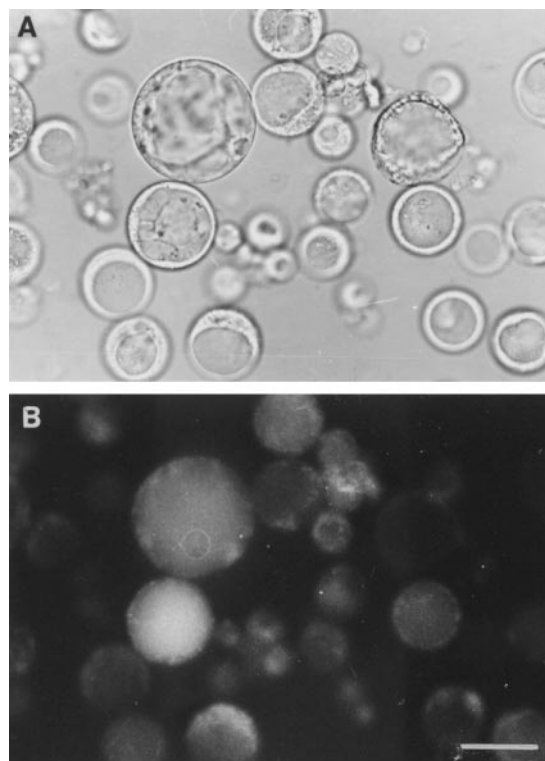


**Figure 1.** Light (A) and fluorescent (B) micrographs of a protoplast preparation isolated from seed coats of bean pretreated with the impermeant sulfhydryl reagent, bromobimane. The bromobimane binds specifically to the plasma membranes of ground parenchyma cells responsible for nutrient efflux from the seed coats (Wang et al., 1995). The protoplasts labeled with the fluorescent tag (B) are characterized by large vacuole that is located off center to give a “thumb-nail” appearance. Bar = 50  $\mu m$ .

solutions (data not shown). Both currents appeared to reverse at membrane voltages ( $V_m$ ) positive of the equilibrium potential for  $K^+$  ( $E_K$ ) and negative of the equilibrium potential for  $Cl^-$  ( $E_{Cl}$ ; Fig. 2, C and D).

### Slowly Activating Outward Current

The slowly activating outward current was observed at membrane voltages ( $V_m$ ) more positive than  $-8 \pm 3$  mV ( $n = 12$ ) in 1 mM KCl external solution. The slowly activating current usually reached a maximum value within 2 to 3 s after the step in  $V_m$  (Fig. 2B). The mean current density of the time-dependent component was  $46.5 \pm 8.5$  mA  $m^{-2}$  ( $n = 30$ ) at 60 mV measured in 1 mM external KCl solution.

The reversal potential ( $E_{rev}$ ) of the slowly activating current was more accurately determined by measuring the “tail current” (Fig. 3A). The  $E_{rev}$  was positive of  $E_K$ , but negative of  $E_{Cl}$  (Fig. 3B), and shifted in the same direction as  $E_K$  in response to a change in external [KCl] (Fig. 3B). The shift of  $E_{rev}$  in response to a 10-fold change in external [KCl] was less than the shift in  $E_K$  (Fig. 3C). The permeability ratio ( $P_K:P_{Cl}$ ) was estimated to be 2.9 from the shift in reversal

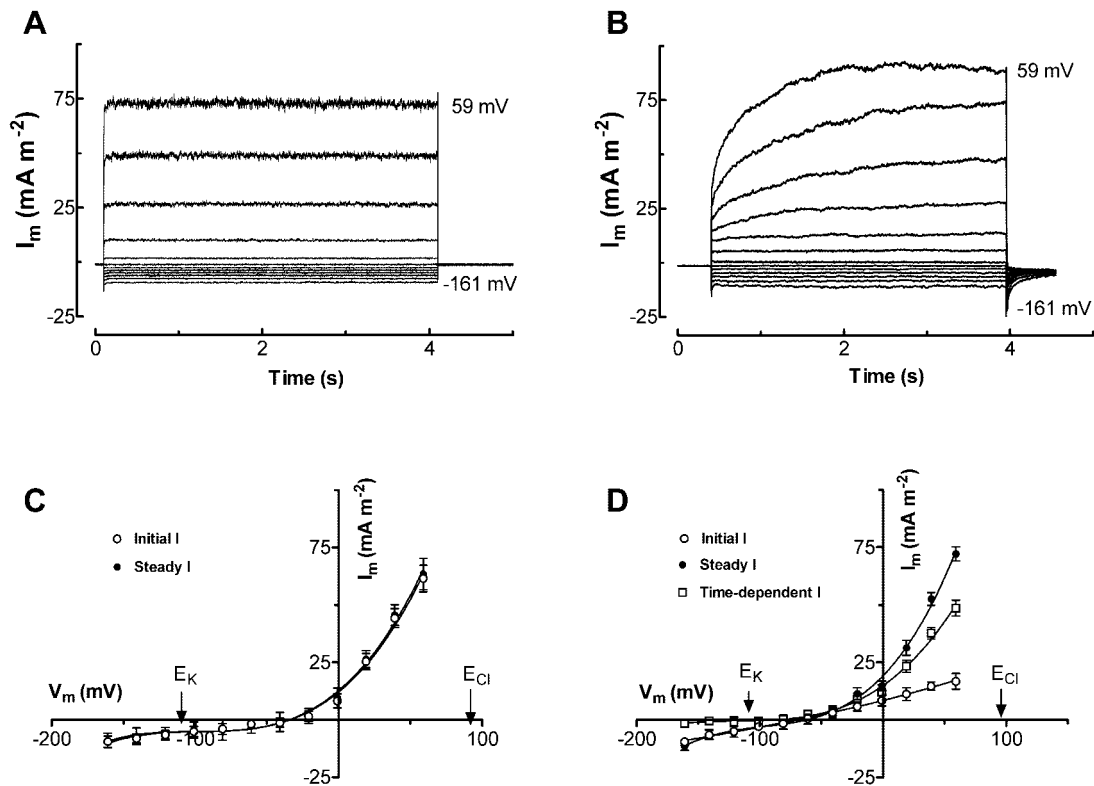


**Figure 2.** Fast-activating (A) and slowly activating (B) outward current elicited by depolarizing voltage pulses from holding potentials of  $-41$  mV to membrane potentials between  $-161$  and  $59$  mV at an increment of  $20$  mV. C and D, Current-voltage curves for protoplasts showing the fast-activating (C) and slowly activating (D) outward currents. Values are means  $\pm$  SE of 14 and 16 protoplasts for C and D, respectively. Pipette solution was type I. Bath solution:  $1$  mM KCl,  $1$  mM  $CaCl_2$ , and  $5$  mM MES [2-(*N*-morpholino)ethanesulfonic acid], pH 6.0.

potential. To examine the  $Ca^{2+}$  selectivity of the current, reversal potentials of tail currents were measured in  $1$  and  $10$  mM  $CaCl_2$  with  $10$  mM KCl in the bath. In  $1$  mM  $CaCl_2$  with  $10$  mM KCl, the reversal potential was  $-23.5 \pm 5.6$  mV ( $n = 8$ ) compared with  $-15.4 \pm 5.1$  mV ( $n = 6$ ) in  $10$  mM  $CaCl_2$  with  $10$  mM KCl. The relative permeabilities  $P_K:P_{Cl}$  and  $P_K:P_{Ca}$  can be calculated using the modified Goldman-Hodgkin-Katz equation and solving it simultaneously for the two cases (MathCad Solve Block, MathSoft, Cambridge, MA). This gives a  $P_K:P_{Cl} = 4.2$  and  $P_K:P_{Ca} = 0.75$ . However, the reversal potentials were not significantly different; therefore,  $P_K:P_{Ca}$  should be considered as a lower limit and  $P_K:P_{Cl}$  as an upper limit. The relative permeabilities for some univalent cations was examined by measuring shifts in reversal potential when the external  $K^+$  was replaced by the same concentration of  $NH_4^+$ ,  $Na^+$ ,  $Cs^+$ ,  $TEA^+$ , or choline<sup>+</sup>. There was a small shift in reversal potential in response to the substitution of  $K^+$  by other univalent cations (Fig. 3D). Based upon the shifts in reversal potential, the permeability sequence relative to  $K^+$  was  $NH_4^+$  ( $0.76 \pm 0.04$ )  $\approx$   $Na^+$  ( $0.74 \pm 0.07$ )  $\approx$   $Cs^+$  ( $0.73 \pm 0.02$ )  $>$   $TEA^+$  ( $0.63 \pm 0.08$ )  $\approx$  choline<sup>+</sup> ( $0.60 \pm 0.10$ ). The permeability sequence of the slowly activating current relative to  $K^+$ , which

was determined by measuring the magnitude of tail current at  $-160$  mV for three protoplasts (Fig. 3D), was  $NH_4^+$  ( $0.69 \pm 0.01$ )  $\approx$   $Na^+$  ( $0.68 \pm 0.02$ )  $>$   $Cs^+$  ( $0.57 \pm 0.03$ )  $>$  choline<sup>+</sup> ( $0.50 \pm 0.03$ )  $\approx$   $TEA^+$  ( $0.45 \pm 0.01$ ). These data show that the transport accounting for the slowly activating current was permeable to univalent cations and  $Ca^{2+}$ , but was selective for  $K^+$  over  $Cl^-$ .

The slowly activating current was not inhibited by  $TEA^+$  or  $Cs^+$ , but was significantly inhibited by  $10$  mM  $Ba^{2+}$  and  $0.1$  mM  $Gd^{3+}$  (Table I). The inhibitory effect of  $Ba^{2+}$  was fully recovered when  $Ba^{2+}$  was removed, whereas  $Gd^{3+}$  inhibition was only partly reversible. No difference in the outward current was found when measured in different activities of external  $Ca^{2+}$  ( $[Ca^{2+}]_o$ ) between  $0.037$  and  $3.6$  mM (data not shown).

#### Fast-Activating Outward Current

We have previously shown that activation and deactivation kinetics of the fast-activating current are best described by a double exponential time course with time constants on the scale of several milliseconds (Zhang et al., 2000). The fast-activating current did not show any inactivation, even during depolar-

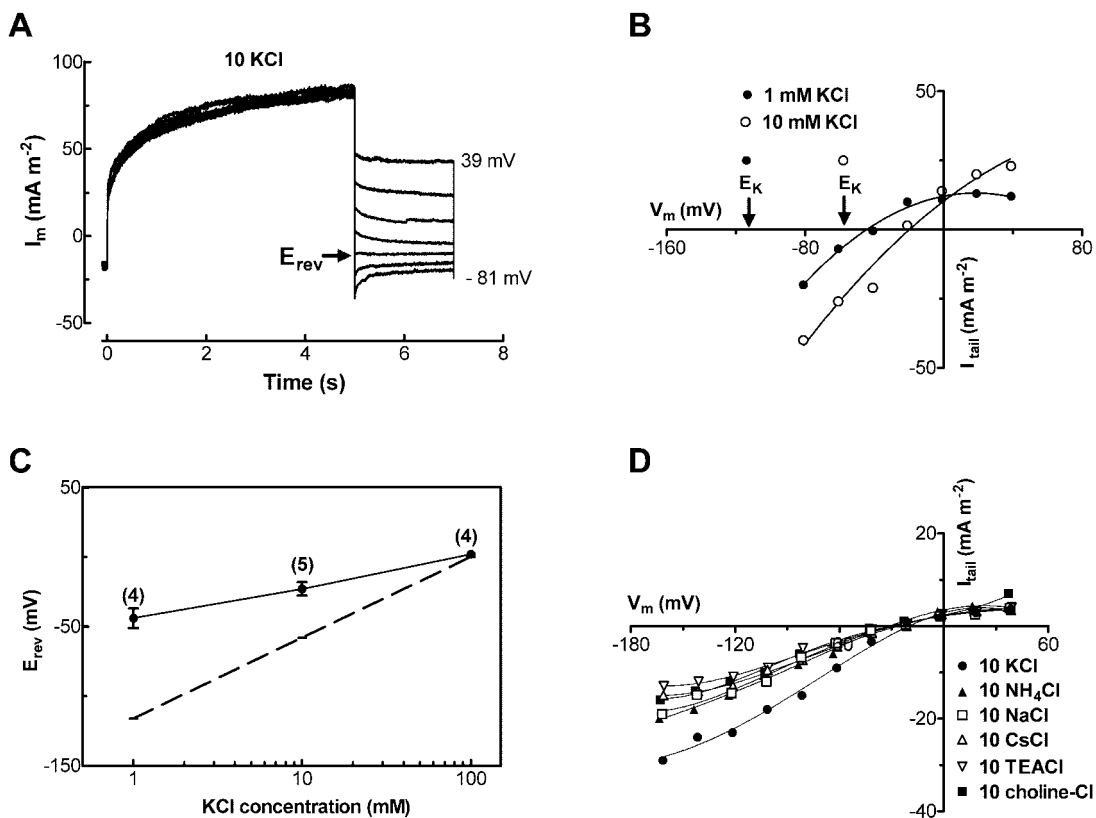


**Figure 3.** Selectivity of slowly activating outward current determined by tail-current measurement. A, The current was activated by stepping the voltage from holding potential of  $-41$  to  $79$  mV and then stepping down to the potentials from  $39$  to  $-81$  mV. Bath solution was:  $10$  mM KCl,  $1$  mM  $\text{CaCl}_2$  and type I pipette solution. B, Tail-current-voltage curves of a protoplast in  $10$  mM and  $1$  mM KCl solutions.  $E_{\text{Cl}}$  was  $54$  and  $89$  mV in  $10$  mM and  $1$  mM KCl solutions, respectively. C,  $E_{\text{rev}}$  plotted as a function of external concentrations of  $\text{K}^+$ . The data were means of protoplasts measured (the number of protoplasts is given in bracket for each point; error bars are the SE). The dashed line represents equilibrium potential for  $\text{K}^+$  ( $E_{\text{K}}$ ). D, Tail current, taken as the difference between the amplitude of the tail current immediately after the decay of the capacitance current and the steady current, plotted against voltages of one protoplast in  $10$  mM cation solutions.

izations that lasted for several minutes (data not shown). The current density of the fast-activating current at  $+60$  mV was  $59.8 \pm 16.2$  mA  $\text{m}^{-2}$  ( $n = 44$ ) in  $1$  mM KCl external solution.

The fast-activating outward current displays weak selectivity for  $\text{K}^+$  over  $\text{Cl}^-$  as determined from tail-current measurements (Zhang et al., 2000). Replacement of external  $\text{Cl}^-$  with Glu had little effect on current magnitude (data not shown) and reversal potential remained relatively unchanged, i.e.  $-1.5 \pm 0.7$  and  $1 \pm 1.2$  mV ( $n = 3$ ) in  $100$  mM KCl and K-Glu bath solution, respectively. Using pulse protocols with a high sampling frequency (i.e.  $10$  kHz), relative permeability was determined by measuring reversal potentials of tail currents. The  $\text{Ca}^{2+}$  selectivity of the current was determined in the same way as for the slow current described above. In  $1$  mM  $\text{CaCl}_2$  with  $10$  mM KCl, the reversal potential was  $-15.7 \pm 3.4$  mV ( $n = 4$ ) compared with  $-16.1 \pm 5.7$  mV ( $n = 4$ ) in  $10$  mM  $\text{CaCl}_2$  with  $10$  mM KCl. From these reversals, a lower limit for  $P_{\text{K}}:P_{\text{Ca}} \cong 4$  and an upper limit of  $P_{\text{K}}:P_{\text{Cl}} \cong 2.5$  is computed. The latter value is in agreement with the previously determined  $P_{\text{K}}:P_{\text{Cl}}$  of  $1.8$

(Zhang et al., 2000). The reversal potential of the tail hardly shifted when the external  $\text{K}^+$  was replaced by  $\text{Cs}^+$ ,  $\text{NH}_4^+$ ,  $\text{Na}^+$ ,  $\text{TEA}^+$ , and  $\text{choline}^+$  (Fig. 4). The selectivity relative to  $\text{K}^+$  calculated from the Goldman-Hodgkin-Katz equation using the shifts in reversal potential observed for three protoplasts was  $\text{Cs}^+$  ( $0.89 \pm 0.15$ )  $\approx$   $\text{NH}_4^+$  ( $0.82 \pm 0.12$ )  $>$   $\text{Na}^+$  ( $0.75 \pm 0.16$ )  $>$   $\text{TEA}^+$  ( $0.62 \pm 0.11$ )  $>$   $\text{choline}^+$  ( $0.53 \pm 0.13$ ). The permeability relative to  $\text{K}^+$  determined from the magnitude of tail current at  $-160$  mV for three protoplasts was  $\text{NH}_4^+$  ( $1.25 \pm 0.11$ )  $>$   $\text{Cs}^+$  ( $0.91 \pm 0.10$ )  $>$   $\text{Na}^+$  ( $0.67 \pm 0.04$ )  $>$   $\text{choline}^+$  ( $0.52 \pm 0.03$ )  $\approx$   $\text{TEA}^+$  ( $0.50 \pm 0.02$ ). These data show that the transport accounting for the fast-activating current was permeable to univalent cations, was selective for  $\text{K}^+$  over  $\text{Ca}^{2+}$ , and was relatively nonselective for cations over anions.

The fast-activating current was insensitive to  $\text{TEA}^+$ ,  $\text{Cs}^+$ ,  $\text{Ba}^{2+}$ , and flufenamate, an antagonist of nonselective cation channels of animal cells (Gorgelein et al., 1990; Table I). However, the current was markedly inhibited by  $\text{Gd}^{3+}$  and  $\text{La}^{3+}$  (Table I). This inhibition was not fully reversed upon removal of

**Table I.** Effect of channel-blockers on the fast-activating outward (FAO), slowly activating outward (SAO), and instantaneous inward (II) currents

The percentage inhibition is given relative to control currents at voltage of +60 mV for outward currents measured in 1 or 10 mM KCl, 1 mM CaCl<sub>2</sub> solutions, and at voltage at -140 mV for instantaneous inward current measured in 100 mM KCl, 1 mM CaCl<sub>2</sub> solution. Values are means ± SE of no. of protoplasts given in brackets.

Blockers	FAO	SAO	II
TEA <sup>+</sup> (10 mM)	98% ± 6% (5)	102% ± 4% (6)	106% ± 9% (4)
Ba <sup>2+</sup> (10 mM)	96% ± 7% (8)	28 ± 7% (3)	94% ± 10% (5)
Ca <sup>2+</sup> (10 mM)	101% ± 6% (10)	97% ± 4% (12)	36% ± 7% (4)
Cs <sup>+</sup> (10 mM)	106% ± 9% (6)	96% ± 8% (5)	98% ± 6% (4)
Gd <sup>3+</sup> (0.1 mM)	21% ± 7% (5)	17 ± 8% (4)	38% ± 12% (5)
La <sup>3+</sup> (0.1 mM)	24% ± 8% (3)	21 ± 6% (3)	35% ± 9% (4)
Flufenamate (0.1 mM)	102% ± 7% (4)	97% ± 5% (3)	96% ± 4% (3)

Gd<sup>3+</sup>. A similar inhibitory effect of La<sup>3+</sup> on the fast-activating current was also observed (Table I).

#### Whole-Cell Inward Current

An "instantaneous" inward current always appeared, because  $V_m$  became more negative than the reversal potentials at low sampling frequencies (Fig. 5A). The current was reduced with decreasing external KCl concentrations, and the reversal potential shifted in the direction of the change in  $E_K$  (Fig. 5B). When hyperpolarizing voltage pulses at sampling frequencies of 10 kHz were applied from holding potential close to the reversal potential, the inward current showed a rapid deactivation (Fig. 5C). Moreover, the fast-activating outward current was elicited by the depolarizing voltage pulses under the same conditions (Fig. 5C). These results suggest that inward current consists of an initial deactivation (partial or complete) of fast outward current that is al-

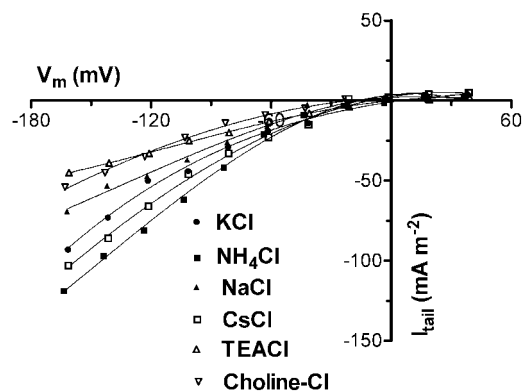


**Figure 4.** Selectivity of the fast-activating outward current determined from measurement of tail-current reversal potential. Tail current, obtained as described in Figure 3 (see also Zhang et al., 2000), plotted as a function of the clamped voltages for one protoplast measured in different monovalent cation solution. Mean results for a number of protoplasts are given in the text. Pipette solution was type I; all bath solution also contained 1 mM CaCl<sub>2</sub> and 5 mM MES, pH 6.0.

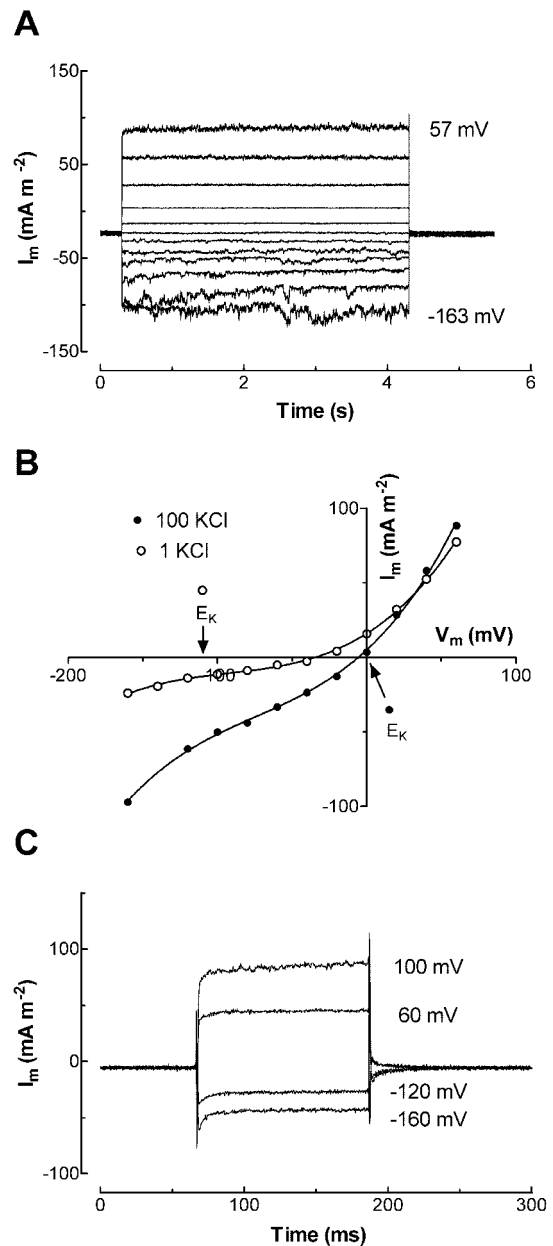


**Figure 5.** Hyperpolarization-activated inward current (A) from a holding potential of -40 mV to  $V_m$  between -160 and 60 mV. Bath solution: 100 mM KCl, 1 mM CaCl<sub>2</sub>, and 5 mM MES, pH 6.0. Pipette solution was type II. B, Initial current-voltage curves for one protoplast measured in 100 and 1 mM KCl solution. C, Activation of fast-activating outward and deactivation of inward current by depolarizing and hyperpolarizing voltage-pulses from holding potential of -40 mV to  $V_m$  shown in the individual current traces. The currents were digitized at 10 kHz and filtered at 2 kHz. Bath solution: 100 mM KCl, 1 mM CaCl<sub>2</sub>, and 5 mM MES, pH 6.0; pipette solution was type I.

ready on at the holding potential. The current that remains after the deactivation may or may not be accounted for by the transport that underlies the fast outward current.

The selectivity of the inward current was examined by substituting 100 mM KCl in the bath with the same

concentration of other univalent cations while maintaining  $[Cl^-]$  constant and measuring the current magnitude at  $-140$  mV. The transport(s) responsible for the inward current were permeable to all the univalent cations examined. The permeability sequence relative to  $K^+$  determined from six to eight protoplasts was:  $NH_4^+$  ( $1.18 \pm 0.37$ )  $> \approx Cs^+$  ( $0.78 \pm 0.11$ )  $\approx Na^+$  ( $0.74 \pm 0.16$ )  $> TEA^+$  ( $0.43 \pm 0.07$ )  $\approx choline^+$  ( $0.39 \pm 0.04$ ).

The inward current was insensitive to  $TEA^+$ ,  $Cs^+$ ,  $Ba^{2+}$ , and flufenamate, but it was inhibited by external  $Ca^{2+}$  and  $Gd^{3+}$  (Table I). It was inhibited to a maximum of approximately 80% by increasing external  $Ca^{2+}$  activity ( $\{Ca^{2+}\}$ ) from  $37 \mu M$  to  $12.6$  mM (Fig. 6, A and B). In contrast, the fast-activating outward current was relatively insensitive to external  $\{Ca^{2+}\}$  (Fig. 6A). The inhibition of the inward current by external  $[Ca^{2+}]$  was independent of  $V_m$ , at least at negative  $V_m$  because the  $EC_{50}$  was not significantly different between  $-60$  and  $-140$  mV (Fig. 6B).

Like the fast-activating outward current, the inward current was sensitive to  $Gd^{3+}$  (Fig. 7A). The

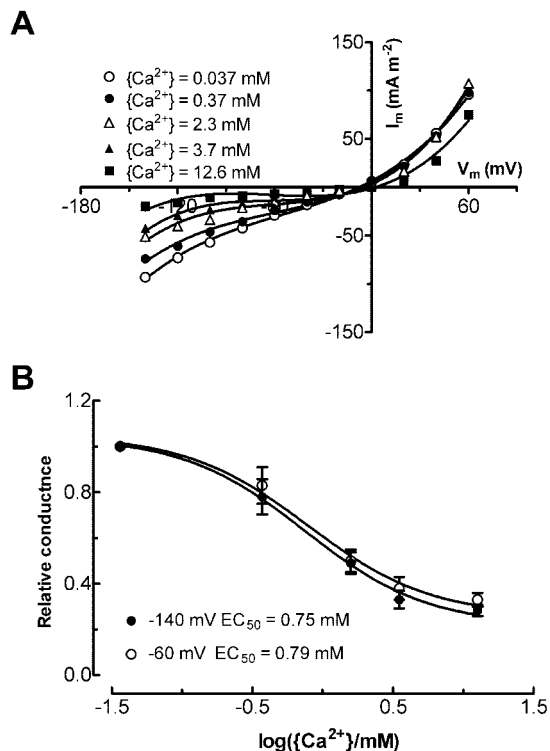


**Figure 6.** Effect of external  $Ca^{2+}$  activity ( $\{Ca^{2+}\}$ ) on fast-activating inward and outward current. Currents were elicited from holding potentials of  $-20$  mV to  $V_m$  between  $-160$  and  $60$  mV in bath solution of  $100$  mM KCl plus a range of  $\{Ca^{2+}\}$ . Pipette solution was type I. A, Initial current-voltage curves for the currents measured in different levels of  $\{Ca^{2+}\}$ . B, Dose-response curves of inhibition of the inward current by  $\{Ca^{2+}\}$  at  $-140$  mV (black circle) and  $-60$  mV (white circle). The half-maximal inhibition value ( $EC_{50}$ ) was estimated from the fitted curve was  $0.75$  and  $0.79$  mM activity for currents at  $-140$  and  $-60$  mV, respectively. Data points are mean  $\pm$  SE of four protoplasts.

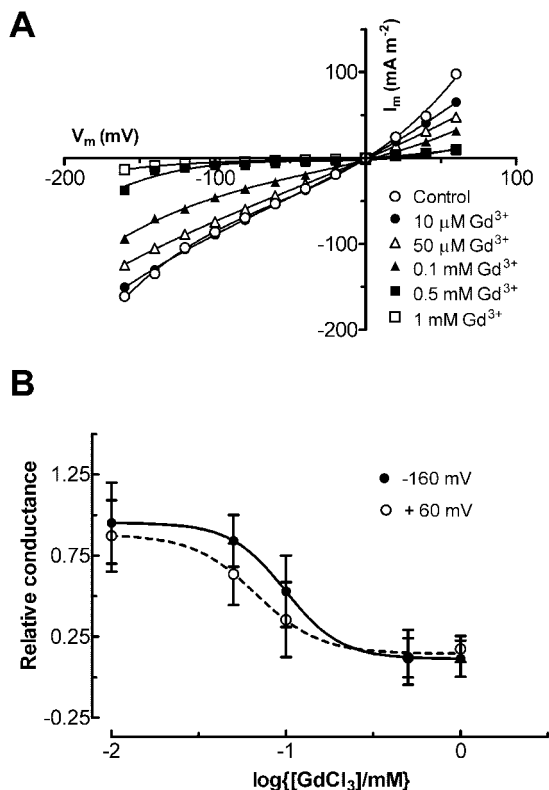


**Figure 7.** Effect of  $GdCl_3$  on the fast-activating current. Currents were elicited from holding potentials of  $-20$  mV to  $V_m$  between  $-160$  and  $60$  mV. A, Initial current-voltage curves before and after addition of varying concentrations of  $GdCl_3$ . All bath solution contained:  $100$  mM KCl,  $1$  mM  $CaCl_2$ , and  $5$  mM MES, pH 6.0; pipette solution was type I. B, Dose-response curves of inhibition of the current by  $GdCl_3$  at  $60$  mV (white circle) and  $-160$  mV (black circle). Data are mean  $\pm$  SE of five protoplasts. The curves were fitted by a Hill equation, giving Hill coefficients of  $2.4$  and  $2.8$  and  $EC_{50}$  values of  $0.70$  and  $0.1$  mM at  $V_m$  of  $-160$  and  $+60$  mV.

dose-response curve for the  $Gd^{3+}$  inhibition was fitted by the Hill equation (Fig. 7B). The Hill slopes were  $2.8$  and  $2.4$  and  $EC_{50}$  values were  $0.1$  and  $0.07$  mM for inward ( $V_m = -160$  mV) and outward ( $V_m = +60$  mV) currents, respectively. The Hill slopes and  $EC_{50}$  values at positive (i.e.  $+60$  mV) and negative (i.e.  $-160$  mV)  $V_m$  values were the same within 95% confidence limits. The inhibitory effect of  $La^{3+}$  on the fast-activating inward and outward currents was similar (Table I).

**Single-Channel Currents**

In some of the outside-out patches, depolarizing voltage pulses induced a time-dependent, slowly activating outward current (Fig. 8A). The current-voltage curves obtained for the initial and final currents were similar to those obtained for the whole-cell configuration when the slow outward current was present (Fig. 8, B and C; compare with Fig. 2D). The time-dependent outward current was best fitted by a single exponential time course with a time

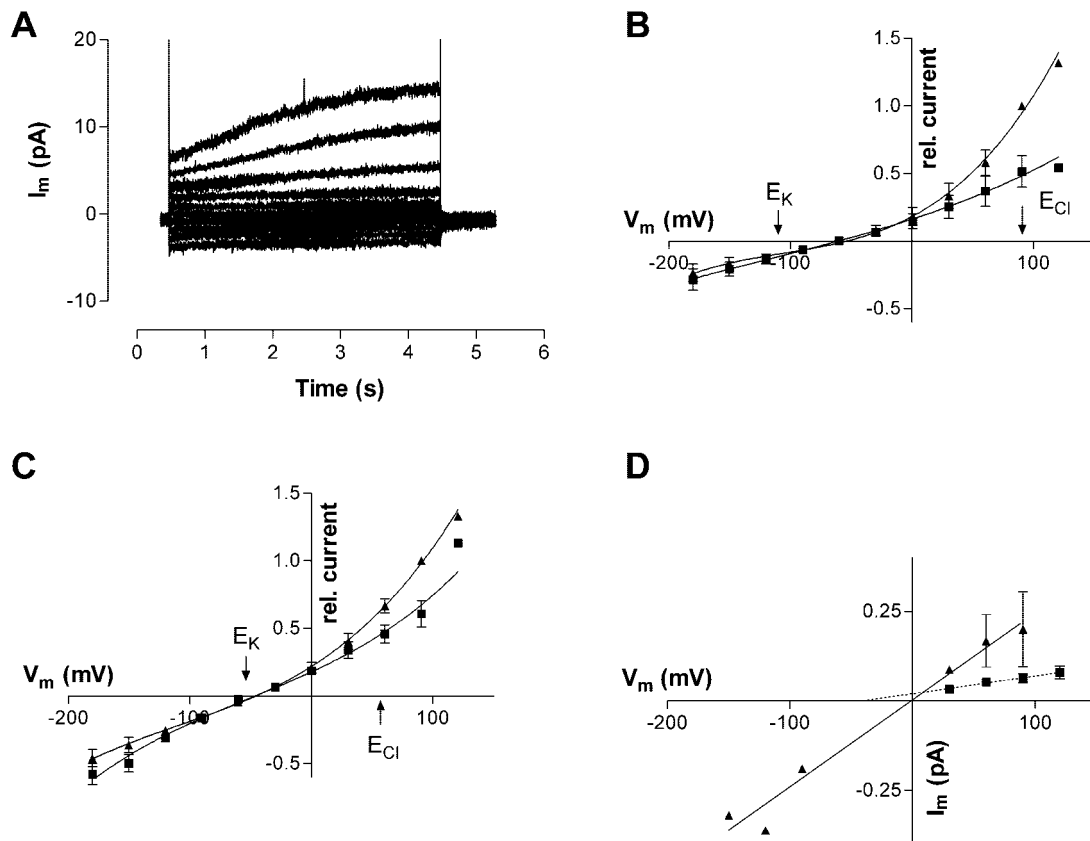


**Figure 8.** Time-dependent slowly activating currents through outside-out patches. A, Current as a function of time in response to voltage clamp pulses from a holding potential of  $-80$  mV to  $V_m$  values between  $-180$  and  $90$  mV at  $30$ -mV increments in  $1$  mM KCl. B and C, Current-voltage curves for initial (■) and final currents (▲) for four patches in  $1$  mM KCl (B) and five patches in  $10$  mM KCl (C). Currents were normalized to the final current at  $90$  mV for each patch. D, Current-voltage curves obtained from nonstationary noise analysis on smooth time-dependent currents obtained from outside-out patches in  $10$  mM KCl (▲,  $n = 4$  patches) or  $1$  mM KCl (■,  $n = 3$  patches). The conductances estimated from linear regressions were  $2.5$  and  $0.5$  pS, respectively. The fitted line for  $1$  mM KCl extrapolates to a reversal potential of  $-40$  mV. The voltage intercept for the  $10$  mM KCl line is  $-1.5$  mV. Bath solution:  $1$  or  $10$  mM KCl,  $1$  mM  $\text{CaCl}_2$ , and  $5$  mM MES; pipette solution was type I. Data were filtered at  $1$  kHz and sampled at  $2$  or  $4$  kHz.

constant of  $2.65 \pm 0.82$  s ( $n = 6$ ) at  $+90$  mV. Distinct individual channel opening and closing events were difficult to resolve for these outward currents. To determine single-channel amplitudes for outward currents, nonstationary noise analysis was used (Heinemann and Conti, 1992; Tyerman et al., 1995). The variance and mean at each time point for 20 to 40 activation curves were obtained, and variance as a function of mean current was plotted. From the initial slope of the fitted curve, the single-channel amplitude for the particular voltage can be obtained. Figure 8D shows the current-voltage curves for  $10$  and  $1$  mM KCl in the bath. The single-channel conductance in  $10$  mM KCl was  $2.4$  pS (95% confidence interval from regression:  $1.86$ – $2.99$  pS,  $n = 4$  patches) and in  $1$  mM KCl it was  $0.49$  pS (95% confidence interval from regression:  $0.32$ – $0.67$  pS,  $n = 3$  patches). The reversal potential in  $10$  mM KCl was close to zero and in  $1$  mM KCl the current-voltage curve extrapolated to  $-40$  mV.

Noisier patch currents that activated rapidly were also observed (Fig. 9A), and single-channel steps could be observed within these (Fig. 9, A and B). In Figure 9B, the single-channel amplitude from nonstationary noise analysis for these fast-activating currents is compared with the amplitude peaks extracted from the same data using the TRAMP analysis technique (Tyerman et al., 1992). The fitted curve in Figure 9B is for 11 Gaussian components with equal separation of  $5.16$  pA, which is the amplitude obtained from the nonstationary noise analysis. It can be seen that at least for the lower amplitudes there is good agreement between the noise analysis and extracted single-channel amplitudes.

Current-voltage curves were obtained with a fast voltage-ramping protocol from which current-voltage curves with channels open were subtracted from those in which one or more channels were closed. These are plotted in Figure 9, C and D, with the current-voltage curves obtained from the noise

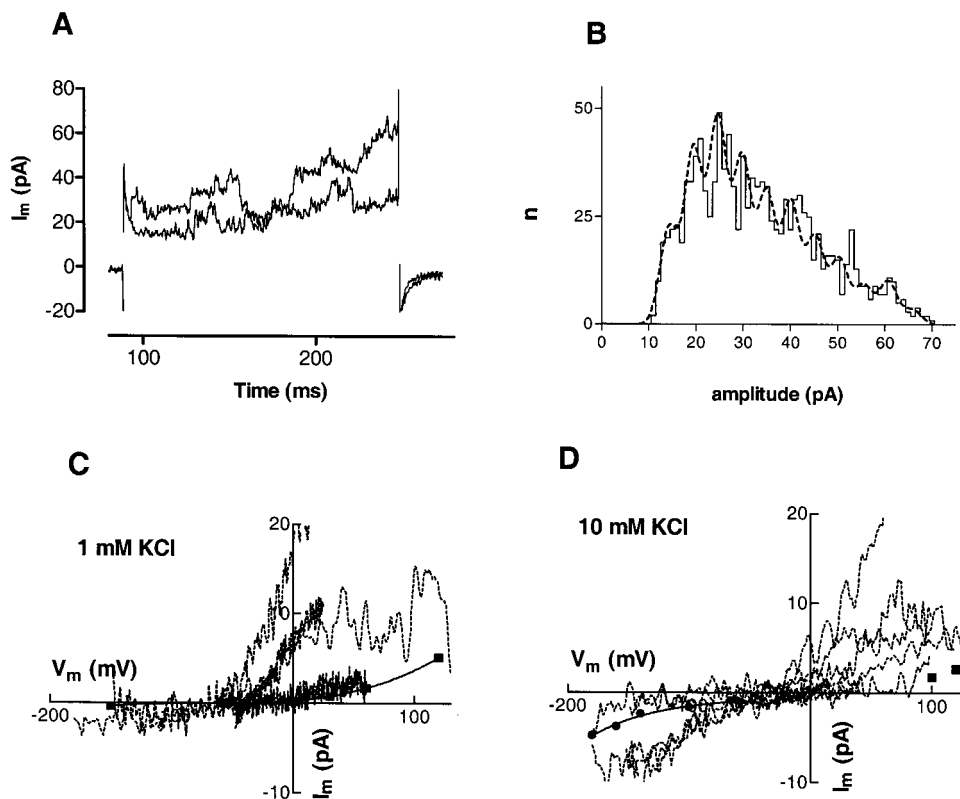


**Figure 9.** Analysis of fast-activating channel currents in outside-out patches. A, Two separate current responses as a function of time illustrating rapid activation of channels subjected to voltage clamp pulses to 120 mV from a holding potential of  $-100$  mV. B, Amplitude histogram (solid line) generated by transition/amplitude (TRAMP) on data such as that shown in A. Current transitions with a  $di/dt$  greater than a threshold value were excluded and mean levels were calculated so long as  $di/dt$  remained below the threshold (Tyerman et al., 1992). Fitted to the data (dotted line) is the sum of 11 Gaussian distributions with the same SD and using the mean current measured using nonstationary noise analysis (5.16 pA) but with variable  $n$ . C and D, Fast voltage ramps were used to obtain current as a function of voltage when channels were open and closed in 1 mM KCl (C, seven patches/ramps) or 10 mM KCl (D, four patches/ramps). The subtracted curves are shown as a function of voltage (dashed lines). Some ramps were from negative to positive voltage where the channel currents captured reversed at the same voltage as for positive to negative going ramps. Also shown are the currents obtained from nonstationary noise analysis (■) with a cubic polynomial regression in A (solid line). Single-channel currents resolved for inward current in 10 mM KCl are also shown for one patch (●) with a fitted cubic polynomial. The external solution contained 1 mM  $\text{CaCl}_2$  and 5 MES, pH 6.0; pipette solution was type I. Data were either filtered at 1 kHz and sampled at 2 kHz or filtered at 2 kHz and sampled at 5 kHz.

analysis (black squares) and also a single-channel record obtained from one patch in which single amplitudes could be clearly recognized at negative membrane potentials (Fig. 9D, black circles). The ramp data gives a range of conductances, which was due mostly to having more than one channel open during a ramp, or channels opening/closing during a ramp (e.g. Fig. 9C at positive  $V_m$ ). The noise analysis data and single-channel data indicate the likely single-channel amplitudes (black symbols) and a single-channel conductance can be estimated at 20 pS near the reversal potential in 10 mM KCl. With 1 mM KCl in the bath (Fig. 9C), the reversal potential of the current-voltage curves from ramps was  $-52.5$  mV ( $SE = 8.2$  mV,  $n = 4$  patches). In 10 mM KCl the mean reversal potential from ramps was  $-19.7$  mV ( $SE = 8.4$  mV,  $n = 7$ ) giving a  $P_K:P_{Cl} = 2.8$ . In two patches where channels were active at negative membrane

potentials, ramps from both positive and negative membrane potentials reversed at the same voltage.

**Effect of Blockers on  $\text{K}^+$  Efflux**

Some of the blockers used in the patch-clamp experiments were also tested on the net release of  $\text{K}^+$  from seed coat halves. The changes in  $\text{K}^+$  efflux relative to controls are presented in Table II.  $\text{Gd}^{3+}$  and  $\text{La}^{3+}$  resulted in about 25% reduction in efflux, whereas  $\text{Ba}^{2+}$  and  $\text{Cs}^+$  resulted in stimulation of the efflux. There was no effect of  $\text{TEA}^+$  or  $\text{Ca}^{2+}$ .

**DISCUSSION**

In response to depolarizing voltage steps, two types of outward current were observed in the whole-cell configuration of protoplasts derived from



**Table II.** Effect of channel blockers on release of potassium from *P. vulgaris* seed coat halves

Data was expressed as percentage of K<sup>+</sup> released compared with control. Four seed coat halves per replicate; corresponding halves between control and treatment washed in 5-mL volumes of bath solution (see Walker et al., 1995); washout solution 300 mOsmol, pH 6 with 5 mM MES; initial 0- to 10-min washout 3 × 3 min, thereafter changed at 10-min intervals.

Treatment	K <sup>+</sup> Efflux % of Control
TEACl (10 mM)	107 ± 5
CsCl (10 mM)	148 ± 8
BaCl <sub>2</sub> (10 mM)	132 ± 9
CaCl <sub>2</sub> (10 mM)	102 ± 4
GdCl <sub>3</sub> (5 mM)	76 ± 3
LaCl <sub>3</sub> (10 mM)	74 ± 3

the ground parenchyma cells of coats of developing bean seeds. The fast-activating outward current occurred ubiquitously, whereas the slowly activating current was present in about 25% of the protoplasts. The two types of outward currents were distinguished by the marked difference in their activation kinetics, with the fast-activating current achieving a steady state approximately 50 times faster than the slowly activating current (Fig. 2; also see Zhang et al., 2000). The currents are unlikely to arise from imperfect seals based upon the time and voltage dependence as well as specific blocker profiles that they displayed. Supporting the notion that channels account for the whole-cell currents, two types of outward rectifying cation channel with distinctly different time activation kinetics were identified in outside-out patches. The channels differed in conductance by an order of magnitude. Both appeared to have a low selectivity between K<sup>+</sup> and Cl<sup>-</sup> that was similar to the selectivity of both types of whole-cell current. The 2.4-pS channel (in 10 mM KCl) activated slowly and could account for the slow outward current observed in whole cells. The more positive reversal potential of this channel also matches with the whole-cell currents under the same ionic gradients, probably reflecting the Ca<sup>2+</sup> permeability of the channel. The 20-pS channel activated rapidly but not as rapidly as the fast outward current observed in whole cells. The 20-pS channel could account for the inward currents observed in whole cells, because it remained activated at negative voltages, allowing inward current flow.

Depolarization-elicited slowly activating K<sup>+</sup> outward rectifiers have been found across a wide variety of plant cell types (Maathuis et al., 1997). Of particular significance to this study is a slowly activating K<sup>+</sup> outward rectifier identified in protoplasts derived from root stelar cells (Wegner and Raschke, 1994; Roberts and Tester, 1995). Recently, an outward rectifier channel gene, cloned from *Arabidopsis*, has been shown by using a knockout mutant to play a central role in loading xylem vessels (Gaymard et al., 1998). Ground parenchyma cells from seed coat per-

form a similar physiological function to root stelar cells. However, the K<sup>+</sup> outward rectifiers in root stelar cells differ in their selectivity and pharmacology from the slowly activating current in bean seed coat ground parenchyma cells. For example, the K<sup>+</sup> outward rectifiers in root stelar cells are highly selective for K<sup>+</sup> and are sensitive to TEA<sup>+</sup> (Wegner and Raschke, 1994; Roberts and Tester, 1995). The slowly activating current observed here seem weakly selective between K<sup>+</sup> and Ca<sup>2+</sup>, nonselective between univalent cations, and insensitive to block by TEA<sup>+</sup> or Cs<sup>+</sup> (compare with Table I). These features of the slowly activating outward current are comparable with a nonselective, slowly activating outward current in xylem parenchyma cells of barley (*Hordeum vulgare*) roots (Wegner and Raschke, 1994; Wegner and De Boer, 1997). The nonselective channel may play a role in transduction of electrical and hydraulic signals because its activity is enhanced at elevated cytoplasmic Ca<sup>2+</sup> activity ( $\{Ca^{2+}\} > 1 \mu M$ ; Wegner and De Boer, 1997). The permeability to Ca<sup>2+</sup> for the slowly activating outward current may also indicate a role in signal transduction. Barium blocked the slowly activating outward current, but had a significant stimulatory effect on the efflux of K<sup>+</sup> from bean seed coat halves, as did Cs<sup>+</sup>. Therefore, it is unlikely that the slowly activating outward current is the pathway for K<sup>+</sup> release in vivo, but it remains a possibility that the current is involved in the control of K<sup>+</sup> release.

A slowly activating outward current observed in outside-out patches is attributed to a 2.4-pS channel. The nonstationary noise analysis used to extract the single-channel characteristics is rarely used in plant ion channel studies but is commonly used in animal studies. Similar time-dependent currents in patches of the symbiosome membrane from soybean nodules are thought to result from a subpicoSiemen channel based upon the noise characteristics of the currents (Tyerman et al., 1995). The subpicoSiemen channel is nonselective for univalent cations (Tyerman et al., 1995), and its rectification is strongly dependent upon Ca<sup>2+</sup> activity on either side of the membrane (Whitehead et al., 1998). It is interesting that the subpicoSiemen channel observed in *Lotus japonicus* symbiosome membrane is also permeable to Ca<sup>2+</sup> (Roberts and Tyerman, 2002), as we have observed in this study for the slow whole-cell currents in bean seed coat cells.

In contrast to the slowly activating current, the fast-activating outward current was less selective between cations and anions ( $P_K:P_{Cl} = 1.8$ ; Zhang et al., 2000) and showed a higher selectivity for K<sup>+</sup> over Ca<sup>2+</sup>. It was nonselective between univalent cations, i.e. K<sup>+</sup> (1.0) ≈ Cs<sup>+</sup> (0.89) ≈ NH<sub>4</sub><sup>+</sup> (0.82) > Na<sup>+</sup> (0.75) > TEA<sup>+</sup> (0.62) > choline<sup>+</sup> (0.53). The selectivity among the univalent cations could be attributed to their different mobilities in aqueous solution: The mobilities relative to K<sup>+</sup> for Na<sup>+</sup> and choline<sup>+</sup> are

0.68 and 0.51, respectively (Robinson and Stokes, 1959). Ion channels with low selectivity between cations and anions are not common in plant cells, but the nonselective channels in barley xylem parenchyma cells exhibit an identical selectivity between  $K^+$  and  $Cl^-$  ( $P_K:P_{Cl} = 1.8$ ; Wegner and De Boer, 1997) to the currents found in the present study. Like the fast-activating currents here, the nonselective channels in xylem parenchyma cells are nonselective for univalent cations, and they exhibit a similar pharmacology.

A hyperpolarization-activated, time-dependent  $K^+$ -selective inward rectifier, which functions to mediate uptake of  $K^+$ , is prominent in higher plant cells (for review, see Maathuis et al., 1997). In contrast, bean seed coats displayed an "instantaneous" inward current at hyperpolarizing  $V_m$ . The following observations suggest that the same channel is responsible for the instantaneous inward and the fast-activating outward current: (a) The instantaneous inward current and the fast-activating outward current always occurred together. (b) They exhibit similar sensitivity to channel antagonists (Table I). (c) Both are nonselective for univalent cations, and they show similar permeability sequences for the univalent cations examined. (d) The instantaneous inward current exhibits a rapid deactivation in response to hyperpolarizing voltage pulses (Fig. 5C). (e) A 20-pS channel appears to be responsible for both inward and outward currents in outside-out patches.

Davenport and Tester (2000) recently characterized a 45-pS channel in plasma membranes of wheat roots by reconstitution in artificial lipid bilayers. This channel, which is suggested to be responsible for the whole-cell nonselective cation current (Tyerman et al., 1997), exhibits high opening probability ( $P_{open}$ ) at depolarized membrane potentials, and the  $P_{open}$  is reduced as the membrane potentials become more negative. Furthermore, this channel is poorly selective between univalent cations, is insensitive to  $TEA^+$ ,  $Cs^+$ , but is inhibited by external  $Ca^{2+}$  and  $Gd^{3+}$  (Davenport and Tester, 2000). These characteristics of channel selectivity and pharmacology are comparable with those of nonselective channels in seed coat ground parenchyma cells. The lack of distinct channel opening and closing events in the majority of outside-out patches at depolarized membrane potentials, but not at hyperpolarized membrane potentials, could be explained by a high  $P_{open}$  at depolarized potentials combined with a large number of channels in the patch. A major difference between the wheat channel and the whole-cell and patch currents from ground parenchyma is the apparent selectivity between  $K^+$  and  $Cl^-$ . The wheat nonselective cation channel in bilayers is highly selective for cations over anions (Davenport and Tester, 2000).

The weak selectivity of the ensemble of channels between  $K^+$  and  $Cl^-$  ions, which are major solutes

released from the seed coats (Walker et al., 1995), will allow efflux of either  $K^+$  or  $Cl^-$  depending on their electrochemical potential differences. Efflux of  $K^+$  from excised bean seed coats is  $71 \text{ nmol m}^{-2} \text{ s}^{-1}$  measured under conditions of zero turgor and no added  $K^+$  in the incubation solution (Patrick, 1984). The  $K^+$  concentration in the seed coat apoplast is estimated to be approximately 1.4 mM under such experimental conditions (Walker et al., 1995). Given the mean diameter of  $30 \text{ }\mu\text{m}$  for the ground parenchyma protoplasts, this  $K^+$  efflux rate corresponds to a current density of  $7 \text{ mA m}^{-2}$ . This current density occurs at membrane potentials of approximately 20 and 50 mV for protoplasts exhibiting only fast or fast and slowly activating outward currents, respectively (Fig. 2, C and D). These membrane potentials are more positive than the  $-100\text{-mV}$  membrane potential measured for intact seed coat cells of zero turgor and bathed in 1 mM KCl (Walker et al., 1995). Because the ensemble of channels responsible for both fast and slow currents are poorly selective for  $K^+$  over  $Cl^-$ , the measured currents at voltages between  $E_K$  and  $E_{Cl}$  will be the net current resulting from efflux of  $K^+$  and  $Cl^-$  from the cell. This may account for some of the discrepancy between seed coat  $K^+$  flux and outward current measured in protoplasts. The observation that  $Cl^-$  efflux is approximately 50% of the  $K^+$  efflux from the excised seed coats of bean (Walker et al., 1995) is consistent with  $P_K:P_{Cl} = 2:1$  for the fast-activating current in ground parenchyma protoplasts. However, the release of  $K^+$  from bean seed coat halves was only inhibited by about 25% using blockers ( $Gd^{3+}$  and  $La^{3+}$ ) that in contrast resulted in almost complete inhibition of inward and outward nonselective cation currents in seed coat protoplasts. This suggests that the nonselective channels described here, particularly the fast-activating current, could only account for about 25% of  $K^+$  release and that there are other transport systems primarily involved in  $K^+$  release that may be electrically silent.

In contrast to bean seed coat,  $K^+$ -selective outward and inward channels predominate in the plasma membranes of transfer cells of *Vicia faba* seed coats (Zhang et al., 1997). Therefore, nonselective channels may not be universal in seed coat unloading or we have patched protoplasts derived from cells with differing transport functions in the two species. There could be a more finely tuned control of solute release from transfer cells of *V. faba* seed coats. For instance, solute turnover in transfer cells of *V. faba* seed coat is about 10-fold greater than that in the ground parenchyma cells of bean seed coat as estimated on seed growth rates and relative cell volume (Patrick, 1994).

The low selectivity of the channel ensemble for a wide range of cations and anions, including large organic ions such as  $TEA^+$ ,  $choline^+$ , and  $Glu^-$ , suggests that the channels seen here may mediate a component of the efflux of phloem-imported ions. It

has been suggested that a nonselective membrane transporter is involved in release of amino acids such as Glu and Lys from pea (*Pisum sativum*) seed coat as deduced from measurement of amino acid influx into excised seed coats (de Jong et al., 1997; van Dongen et al., 2001). The nonselective nature of the ensemble of channels and their activation over a wide range of membrane potentials (Zhang et al., 2000) may ensure that all nutrient ions imported from the phloem can flow into the seed apoplast. A low-resistance pathway for nutrient ions through the channel ensemble would enable the ground parenchyma cells to keep a low turgor pressure, thus maintaining a constant hydrostatic pressure difference between source and sink. This would in turn allow for a sustained phloem import into the seed coat.

## MATERIALS AND METHODS

### Plant Materials and Protoplast Isolation

Plants of bean (*Phaseolus vulgaris* L. cv Redland pioneer) were raised and seeds harvested for isolating protoplasts as described previously (Wang et al., 1995). Seed coat halves of bean were cut longitudinally into small pieces and digested with enzyme solution of 0.8% (w/v) cellulase (Onozuka RS, Yakult Honsha, Tokyo) and 0.08% (w/v) pectolyase (Sigma, St. Louis) for 2 to 3 h at 20°C. A Suc density gradient, as described previously (Zhang et al., 1997), was used to collect clean protoplasts. The protoplasts were kept on ice until patch clamped. Protoplasts of ground parenchyma cells that function to release solutes were identified on the basis of their characteristic appearance (Fig. 1). The mean diameter of these protoplasts was  $29.2 \pm 4.3 \mu\text{m}$  (SD,  $n = 86$ ).

### Electrophysiology and Data Analysis

Patch pipettes, pulled from borosilicate glass blanks (Clark Electromedical, Readings, UK), were coated with Sylgard<sup>R</sup> (Dow Corning, Midland, MI). Voltage across the patch was controlled and current measured using an Axopatch 200B (Axon Instruments, Foster City, CA). Whole-cell preparations were obtained by forming a gigaseal in the cell-attached mode and then applying a short burst of extra suction to rupture the membrane. Successful achievement of whole-cell configuration was indicated by a substantial increase in capacitance. Series resistance was compensated to about 50% and capacitance was compensated. Voltage pulses between 60 ms and 4 s in duration were used to study the voltage-dependent current. Data was sampled at either 2 or 10 kHz and filtered at 0.5 and 2 kHz, respectively, by a low-pass 4-pole Bessel filter. Sufficient time between voltage pulses was given to allow currents to settle to a steady-clamp current for the particular holding potential before a new pulse was applied. Records were stored and analyzed using pClamp 6.0 (Axon Instruments, Foster City, CA). All experiments were carried out at room temperature (20°C–22°C). Junction potentials were calcu-

lated and corrected for using the program JPCalc (P.H. Barry, University of New South Wales, Sydney).

Current-voltage curves from whole-cell recordings were constructed from a series of voltage steps. "Initial current," measured approximately 2 or 50 ms after the beginning of voltage pulses for short and long voltage-pulses, and "final current," measured at the end of voltage pulses, were used to construct current-voltage curves. Current-voltage curves were fitted with third order polynomials. Single-channel data were recorded from outside-out patches formed from whole-cell configuration after pulling the patch-pipette off the protoplast. A fast voltage ramping protocol was used to obtain the current-voltage curve for single channels (Tyerman and Findlay, 1989). Nonstationary noise analysis was applied to time-dependent currents in outside-out patches according to Heinemann and Conti (1992). Single-channel amplitudes were determined using TRAMP analysis (Tyerman et al., 1992).

### Experimental Solutions

Two types of pipette solution were commonly used in the present study. They were composed of type I (high Cl<sup>-</sup>), 100 mM KCl, 2.3 mM CaCl<sub>2</sub>, 2 mM MgCl<sub>2</sub>, 2 mM Na<sub>2</sub>ATP, 10 mM EGTA, and 10 mM HEPES [4-(2-hydroxyethyl)-1-piperazineethanesulfonic acid]; and type II (low Cl<sup>-</sup>), 10 mM KCl, 90 mM K-Glu, 2.3 mM CaCl<sub>2</sub>, 2 mM MgCl<sub>2</sub>, 2 mM Na<sub>2</sub>ATP, 10 mM EGTA, and 10 mM HEPES. Free calcium concentrations of both types of pipette solution were approximately 50 nM calculated using the chemical speciation program GEOCHEM (Parker et al., 1987). Both solutions were adjusted to osmolality of 720 mOsm with sorbitol and pH 7.2 with Tris. All bath solutions contained in addition to other solutes: 1 mM CaCl<sub>2</sub>, 5 mM MES, pH 6.0, and 700 mOsm kg<sup>-1</sup> adjusted with Tris and sorbitol, respectively. The details of the bath and pipette solutions are given in appropriate figure legends. Ionic activities, computed using the program GEOCHEM (Parker et al., 1987), were used and are given in the relevant figure legends.

### ACKNOWLEDGMENTS

We thank Louise Hetherington and Wendy Sullivan for their expert technical assistance and Kevin Stokes for supplying experimental plant materials. We thank two anonymous reviewers for their suggestions.

Received June 26, 2001; returned for revision August 13, 2001; accepted October 21, 2001.

### LITERATURE CITED

Buschmann PH, Vaidyanathan R, Gassmann W, Schroeder JI (2000) Enhancement of Na<sup>+</sup> uptake currents, time-dependent inward-rectifying K<sup>+</sup> channel currents, and K<sup>+</sup> channel transcripts by K<sup>+</sup> starvation in wheat root cells. *Plant Physiol* **122**: 1387–1397

- Davenport RJ, Tester M** (2000) A weakly voltage-dependent, non-selective cation channel mediates toxic sodium influx in wheat. *Plant Physiol* **122**: 823–834
- de Jong A, Koerselman-Kooij JW, Schuurmans AMJ, Bostlap AC** (1997) The mechanism of amino acid efflux from seed coats of developing pea seeds as revealed by uptake experiments. *Plant Physiol* **114**: 731–736
- Gaymard F, Pilot G, Lacombe B, Bouchez D, Bruneau D, Boucherez J, Michaux-Ferriere N, Thibaud J-B, Sentenac H** (1998) Identification and disruption of a plant shaker-like outward channel involved in K<sup>+</sup> released into the xylem sap. *Cell* **94**: 647–655
- Gorgelein H, Dahlem D, Englem HC, Lang HJ** (1990) Flufenamic acid, memfenamic acid and niflumeic acid inhibits single non-selective cation channels in the rat exocrine pancreas. *FEBS Lett* **268**: 79–82
- Heinemann SH, Conti F** (1992) Nonstationary noise analysis and application to patch clamp recordings. *Methods Enzymol* **207**: 131–148
- Maathuis FJM, Ichida AM, Sanders D, Schroeder JI** (1997) Roles of higher plant K<sup>+</sup> channels. *Plant Physiol* **114**: 1141–1149
- Offler CE, Patrick JW** (1984) Cellular structures, plasma membrane surface areas and plasmodesmatal frequencies of seed coats of *Phaseolus vulgaris* L. in relation to photosynthate transfer. *Aust J Plant Physiol* **11**: 79–100
- Parker DR, Zelazny LW, Kinraide TB** (1987) Improvements to the program GEOCHEM. *Soil Sci Soc Am J* **51**: 488–491
- Patrick JW** (1984) Photosynthate unloading from seed coats of *Phaseolus vulgaris* L.: control by water relations. *J Plant Physiol* **115**: 297–310
- Patrick JW** (1994) Turgor-dependent unloading of assimilates from coats of developing legume seed: assessment of the significance of the phenomenon in the whole plant. *Physiol Plant* **90**: 645–654
- Patrick JW, Offler CE** (1995) Post-sieve element transport of sucrose in developing seed. *Aust J Plant Physiol* **22**: 681–702
- Roberts DM, Tyerman SD** (2002) Voltage-dependent cation channels permeable to NH<sub>4</sub><sup>+</sup>, K<sup>+</sup>, and Ca<sup>2+</sup> in the symbiosome membrane of the model legume *Lotus japonicus*. *Plant Physiol* **128**: 370–378
- Roberts S, Tester M** (1995) Inward and outward K<sup>+</sup> selective currents in the plasma membrane of protoplasts from maize root cortex and stele. *Plant J* **8**: 811–825
- Roberts S, Tester M** (1997) A patch clamp study of Na<sup>+</sup> transport in maize roots. *J Exp Bot* **48**: 431–440
- Robinson RA, Stokes RM** (1959) *Electrolyte Solutions*. Butterworth, London
- Tyerman SD, Findlay GP** (1989) Current-voltage curves of single Cl<sup>-</sup> channels which coexist with two types of K<sup>+</sup> channels in the tonoplast of *Chara corallina*. *J Exp Bot* **40**: 105–117
- Tyerman SD, Skerrett M, Garrill A, Findlay GP, Leith RA** (1997) Pathways for the permeation of Na<sup>+</sup> and Cl<sup>-</sup> into protoplasts derived from the cortex of wheat roots. *J Exp Bot* **48**: 459–480
- Tyerman SD, Terry BR, Findlay GP** (1992) Multiple conductances in the large K<sup>+</sup> channel from *Chara corallina* shown by transient analysis method. *Biophys J* **61**: 736–739
- Tyerman SD, Whitehead LF, Day DA** (1995) A channel-like transporter for NH<sub>4</sub><sup>+</sup> on the symbiotic interface of N<sub>2</sub>-fixing plants. *Nature* **378**: 629–632
- van Dongen JT, Laan RGW, Wouterlood M, Borstlap AC** (2001) Electrodifusional uptake of organic cations by pea seed coats: further evidence for poorly selective pores in the plasma membrane of seed coat parenchyma cells. *Plant Physiol* **126**: 1688–1697
- Walker NA, Patrick JW, Zhang WH, Fieuw S** (1995) Efflux of photosynthate and acid from developing seed coats of *Phaseolus vulgaris* L.: a chemiosmotic analysis of pump-driven efflux. *J Exp Bot* **45**: 597–697
- Walker NA, Zhang WH, Harrington G, Holdaway N, Patrick JW** (2000) Effluxes of solutes from developing seed coats of *Phaseolus vulgaris* L. and *Vicia faba* L.: locating the effects of turgor in a coupled chemiosmotic system. *J Exp Bot* **51**: 1047–1055
- Wang X-D, Harrington G, Patrick JW, Offler CE, Fieuw S** (1995) Cellular pathways of photosynthate transport in coats of developing seed of *Vicia faba* L. and *Phaseolus vulgaris* L.: principal cellular sites of efflux. *J Exp Bot* **45**: 49–63
- Wegner LH, De Boer AH** (1997) Properties of two outward-rectifying channels in root xylem parenchyma cells suggest a role of in K<sup>+</sup> homeostasis and long distance signaling. *Plant Physiol* **115**: 1707–1719
- Wegner LH, Raschke K** (1994) Ion channels in the xylem parenchyma of barley roots. *Plant Physiol* **105**: 799–813
- White PJ, Lemtiri-Chlieh F** (1995) Potassium currents across the plasma membrane of protoplasts derived from rye roots: a patch-clamp study. *J Exp Bot* **45**: 497–511
- Whitehead LF, Day DA, Tyerman SD** (1998) Divalent cation gating of an ammonium permeable channel in the symbiotic membrane from soybean nodules. *Plant J* **16**: 313–324
- Zhang WH, Walker NA, Patrick, Tyerman SD** (1997) Mechanism of solute efflux from seed coat: whole-cell K<sup>+</sup> currents in the plasma membrane of protoplasts derived from *Vicia faba* L. seed coats. *J Exp Bot* **48**: 1565–1572
- Zhang WH, Walker NA, Tyerman SD, Patrick JW** (2000) Fast activation of a time-dependent outward current in protoplasts derived from coats of developing *Phaseolus vulgaris* seeds. *Planta* **211**: 894–898